



Extreme Value-Based Methods for Modeling Elk Yearly Movements

Dhanushi A. WIJEYAKULASURIYA, Ephraim M. HANKS, Benjamin A. SHABY, and Paul C. CROSS

Species range shifts and the spread of diseases are both likely to be driven by extreme movements, but are difficult to statistically model due to their rarity. We propose a statistical approach for characterizing movement kernels that incorporate landscape covariates as well as the potential for heavy-tailed distributions. We used a spliced distribution for distance travelled paired with a resource selection function to model movements biased toward preferred habitats. As an example, we used data from 704 annual elk movements around the Greater Yellowstone Ecosystem from 2001 to 2015. Yearly elk movements were both heavy-tailed and biased away from high elevations during the winter months. We then used a simulation to illustrate how these habitat effects may alter the rate of disease spread using our estimated movement kernel relative to a more traditional approach that does not include landscape covariates.

Supplementary materials accompanying this paper appear online.

Key Words: Animal movement; Disease spread; Resource selection; Heavy-tailed; MCMC.

1. INTRODUCTION

Brucellosis is a zoonotic disease caused by the bacteria, *Brucella abortus*, which was introduced by cattle to wildlife in the Greater Yellowstone Ecosystem (GYE) during the initial European settlement (Meagher and Meyer 1994). From 1998 to 2016, there have been 27 affected livestock herds, all of which were likely to have been infected from elk (National Academies of Sciences, Engineering, and Medicine 2017; Kamath et al. 2016). The transmission of brucellosis is highest in March through May due to abortion events (Cross et al. 2015). Our goal is to model winter-to-winter elk yearly movements and use estimates of movement rates to better understand how landscape features and extreme movements affect connectivity of GYE elk. We used data provided by State and Federal agencies

Dhanushi A. Wijeyakulasuriya (⋈) and · Ephraim M. Hanks · Benjamin A. Shaby · Department of Statistics, Pennsylvania State University, University Park, PA 16802, USA (E-mail: dzw5320@psu.edu). Benjamin A. Shaby, Institute for CyberScience, Pennsylvania State University, University Park, PA 16802, USA. Paul C. Cross, U.S. Geological Survey, Northern Rocky Mountain Science Center, Bozeman, MT 59715, USA.

^{© 2018} International Biometric Society

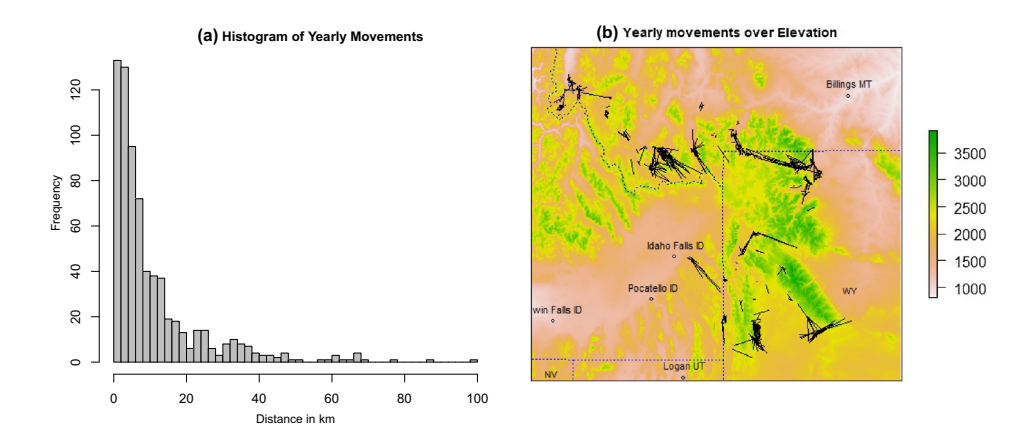


Figure 1. 704 elk movements from one winter to the next around the Greater Yellowstone Ecosystem in Montana, Wyoming and Idaho. The data were both heavy-tailed (a) and biased toward some landscape features like elevation (b).

around the GYE on 521 unique elk over 704 yearly elk movements from 2001-2015. One of the individuals in the dataset was a male. We included his movement in the analysis for completeness, but as there was only one male, we chose not to directly model any differences in movement behavior between male and female elk. A single elk was included at most three times in the data, and we considered each year of data to be independent samples of annual elk movements. We identified all elk with telemetry locations in the months of January–February of two successive years. The temporal resolution of the elk telemetry data varied, with fixes occurring at intervals ranging from 1 to 9 days. For each elk, we identified the telemetry location closest to January 1st of each year but not later than February. A single yearly movement was a pair of such points from consecutive years for a single elk. We see that in these data yearly movements appear to show a heavy tail, with most year-to-year movements less than 40 km, but with a handful of extreme movements observed up to 100 km (Fig. 1a).

In addition to these data, we created grids of agricultural land, forest cover and water from the National Land Cover Database. We rasterized private land polygons obtained from Surface Management Agency spatial data. We created a grid of primary and secondary roads from Transportation Investment Generating Economic Recovery (TIGER). We used a digital elevation map for elevation and terrain roughness. The raster and movement data are freely available on ScienceBase.gov (https://doi.org/10.5066/P9CN4X34). We aggregated the original rasters by a factor of four to improve computational efficiency and interpolated any missing values (see Appendix A). The annual movements are in Fig. 1b) mapped over the raster layer Elevation. The 8 raster layers are shown in Fig. 2. The R package raster (Hijmans 2016) was used in handling the raster layers. We converted the raster layers as well as the movement data from longitude and latitude coordinates to UTM coordinates prior to analysis.

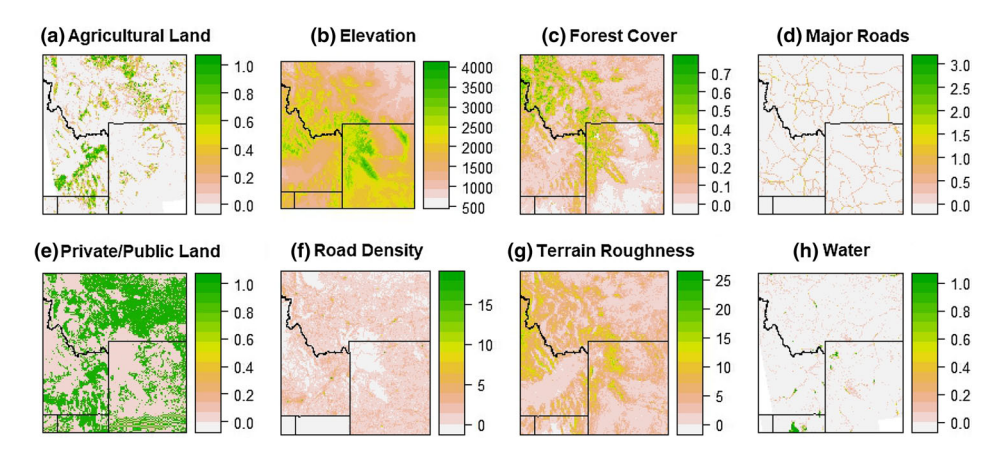


Figure 2. Landcover raster layers.

An individual yearly elk movement is the sample unit, and the desired inference is at the population level. That is, we are most interested in population-level understanding of movements from year to year, and the individuals are assumed to be samples from the population of elk.

Our goal is to model the yearly movement of elk incorporating both resource selection and any heavy-tailed behavior in movements. To our knowledge, previous studies have not addressed both these issues in a single, unified approach. We illustrate how implementing this approach leads to important insights about the relative speed of disease invasion in different habitat structures due the effect of landscape covariates on the movement kernel. Morales (2002) discusses how behavior over patchy terrain can produce leptokurtic movement distributions. Jointly modeling heavy-tailed movements and resource selection will allow us to better understand the relative importance of these two processes.

2. THE RESOURCE SELECTION MODEL

Resource selection models (RSMs) consider a weighted distribution formulation of a point process model to model-independent individual locations. These models seek inference concerning the preference that individuals make given the type of environment. The use of "resources" by the individual is explicitly modeled by a nonnegative function that influences the spatial density of individual locations (Hooten et al. 2017).

A wide variety of models that fall into the area of resource selection are discussed in Johnson et al. (2008) which proposes a general framework for analyzing telemetry data. Coulon et al. (2008) modeled a step selection function (SSF) that represented the probability of selecting a given movement as a function of landscape variables and distance travelled. SSFs are similar to RSMs except that while RSMs analyze locations of animals independently, SSFs analyze the segments separating the successive locations (Coulon et al. 2008). Forester et al. (2009) proposed a model for a SSF that includes a resource selection function and a resource-independent movement kernel. An exponential distance kernel and a spline function were used to model distance. This form makes parameter estimation straightfor-

ward but is unable to capture heavy-tailed movements. Avgar et al. (2016) propose a model that simultaneously models resource selection as well as movement through time. However, we are not interested in modeling temporal correlation in the data since we have at most three time points for each elk, which we assume to be independent of one another.

Resource utilization function (RUF) models (Marzluff et al. 2004) are similar in concept to RSMs but use a two-step approach. In the first step, the density of space use is estimated over the region of interest and in the next step the output of step 1 is linked to a set of spatial covariates in a regression model. For a comparison of RUF and RSF models, see Hooten et al. (2013). In this study, we look at yearly movements independently and do not consider the time component since we do not have sufficient data for individual elk over multiple years. However, there is a rich body of literature for modeling animal movement in time. Point process models are straightforward when the goal is resource selection inference. When the temporal component is included explicitly, these models become increasingly more involved. Instead of point process models, it is more common to model temporally dependent telemetry data using discrete-time dynamic models (Morales et al. 2004; McClintock et al. 2012). These models allow for explicit modeling of the temporal dependence (Hooten et al. 2017). When measurement error is formally accounted for in these models, they are commonly called state space models.

Hooten et al. (2017) argue that discrete-time models have their advantages as they can borrow from well-established tools in time series literature, model dynamics can be easily thought of in discrete time, and discretizing is needed at some level when implementing these models digitally. However, movement is inherently a process that happens in continuous space and time. Continuous-time processes conceptually consider time to be continuous, although some discretizing may occur when implementing these models (Hooten et al. 2010; Hanks et al. 2015). McClintock et al. (2014) review both discrete- and continuous-time models and discuss the similarities and differences between them, giving guidance as to under which circumstances one type of model is preferable over the other. For the elk data we consider here, we do not consider temporal dependence, as the data are year-to-year movements. As each year's movement can be reasonably assumed to be independent, our model will be most similar to RUFs and SSFs.

We consider the following form of a resource selection model. Let $(\mathbf{s}_i, \mathbf{e}_i)$ be the *i*th movement, where \mathbf{s}_i and \mathbf{e}_i are the coordinates of the start and end locations given in terms of UTM coordinates. We consider an RSM based on a weighted distribution (Johnson et al. 2008). The model for the *i*th observation has the following form

$$[\mathbf{e}_{i} \mid \mathbf{s}_{i}] = \frac{e^{\mathbf{x}_{i}'(\mathbf{e}_{i})\boldsymbol{\beta}}q(\mathbf{e}_{i}; \mathbf{s}_{i}, \boldsymbol{\theta})}{\int_{S} e^{\mathbf{x}'(\mathbf{z})\boldsymbol{\beta}}q(\mathbf{z}; \mathbf{s}_{i}, \boldsymbol{\theta})d\mathbf{z}}$$
(1)

where $\mathbf{x}(\mathbf{e}_i)$ denotes the features of the *i*th end location, the bracket notation denotes a probability density function, and $\boldsymbol{\beta}$ is the coefficients associated with the landscape features. The integral in the denominator is over the study region $S \in \mathbb{R}^2$ which has compact support. $q(\mathbf{z}; \mathbf{s}_i, \boldsymbol{\theta})$ is the density of the end location \mathbf{z} . It is of the form

$$q(\mathbf{z}; \mathbf{s_i}, \boldsymbol{\theta}) = \frac{1}{2\pi} \frac{1}{||\mathbf{z} - \mathbf{s}_i||} f(||\mathbf{z} - \mathbf{s}_i||).$$

Let f be the density of the distance kernel. Let d and φ be distance travelled and bearing, respectively, each distributed as $d \sim f$ and $\varphi \sim U(0, 2\pi)$. Let (s_1, s_2) be the UTM coordinates of the start location and (z_1, z_2) be the UTM coordinates of the end locations. We can obtain (z_1, z_2) as $z_1 = s_1 + d\cos(\varphi)$ and $z_2 = s_2 + d\sin(\varphi)$. The joint density for $\mathbf{z} = (z_1, z_2)$, which we denote as $q(\mathbf{z}; \mathbf{s_i}, \boldsymbol{\theta})$ above, is obtained using standard change-of-variable methods.

We hypothesized that elk prefer medium elevation values in winter months, and therefore, we include a quadratic term for this covariate to capture such a preference. We consider only linear terms for all other landscape features. Other functional forms of the covariates can be easily incorporated into this model. However, finding the best possible combination of covariates is not the primary goal of this paper. The function f is the density kernel for the Euclidean distance $||\mathbf{e}_i - \mathbf{s}_i||$ computed in kilometers. We compare two functional forms for f in this study. We first consider a Gamma kernel, which is a distance kernel with a light tail. We then consider a distance kernel with a flexible tail defined by standard extreme value theory (EVT) models.

EVT is a theoretical framework for modeling extremes of data and has been used in many scientific disciplines like hydrology and climatology. However, the use of EVT in ecology and specifically in modeling heavy-tailed movement is limited. Garcí-a and Bordade Água (2017) claim to be the first to use EVT methods in modeling plant dispersal. One of the initial proponents of capturing long-range dispersals was Kot et al. (1996) who used integro-difference equations to model the spread of invading organisms. These models were extended to a mixed model by Clark (1998) who applied these methods to the invasion of different tree species at the end of Pleistocene. A drawback of these models is that the tail parameters were not estimated; only model comparison was done between models. Clark et al. (1999) suggested a model which overcame this drawback by using a two-dimensional t distribution to model the dispersal kernel. Clark et al. (2003) proposed a new stochastic model which used a Bayesian framework and modeled the dispersal kernel as a discrete multinomial distribution. Clark et al. (2003) also state that classical diffusion models are more useful in modeling animal dispersal than plant dispersal and that long distance dispersal events are less common in animal dispersals. However, our data show evidence of long-range movements for elk winter-to-winter and therefore we are interested in capturing any such extreme movements.

We consider a distance kernel obtained by splicing a Gamma distribution and a generalized Pareto distribution (GPD) together. This spliced distribution is flexible enough to capture a wide range of tail behavior, including heavy and light tailed movements. Pairing this with the RSM (1) results in a flexible model that allows for both resource selection and heavy-tailed dispersal.

2.1. THE GAMMA DISTANCE KERNEL

The Gamma distance kernel has the following form

$$h(d \mid k, \theta) = \frac{1}{\Gamma(k)\theta^k} d^{k-1} e^{-\frac{x}{\theta}}$$
 (2)

where k and θ are the shape and scale parameters, respectively, and Γ is the Gamma function. The Gamma distance kernel has a light tail, and this may not account for extreme movements of elk.

2.2. THE SPLICED DISTANCE KERNEL

We consider two forms for a spliced distribution where the functional form of the distance kernel f takes different forms below and above a threshold u. MacDonald et al. (2011) suggested modeling the CDF of the spliced kernel as

$$F(d \mid k, \theta, \sigma, \xi, \phi_u) = \begin{cases} \frac{1 - \phi_u}{H(u \mid k, \theta)} H(d \mid k, \theta) & \text{for } d \leq u, \\ (1 - \phi_u) + \phi_u G(d \mid \sigma, \xi) & \text{for } d > u. \end{cases}$$
(3)

Here, u denotes the threshold and $\phi_u = Pr(d > u)$ is the tail fraction: the probability mass above u. H is the CDF of the "bulk model," which models yearly movements shorter than u. We model H as a Gamma distribution with shape and scale parameters k and θ , respectively. G is the CDF of the tail model, which we model as a GPD with shape and scale parameters ξ and σ . The form of the PDF is

$$f(d \mid k, \theta, \sigma, \xi, \phi_u) = \begin{cases} \frac{1 - \phi_u}{H(u \mid k, \theta)} h(d \mid k, \theta) & \text{for } d \le u, \\ \phi_u g(d \mid \sigma, \xi) & \text{for } d > u. \end{cases}$$
(4)

where h and g are the Gamma and GPD densities, respectively. The GPD density g has the following form

$$g(d \mid \sigma, \xi) = \frac{1}{\sigma} \left(1 + \frac{\xi(d-u)}{\sigma} \right)^{\left(-\frac{1}{\xi} - 1\right)}$$
 (5)

with the constraint that $d \ge u$ when $\xi \ge 0$, and $u \le d \le u - \sigma/\xi$ when $\xi < 0$. The scale parameter σ is constrained to be positive, and the shape parameter ξ controls the heaviness of the tail of the movement kernel, where $\xi > 0$, $\xi < 0$ and $\xi = 0$ correspond to a heavy tail, finite tail and a light tail, respectively.

Specifying the tail fraction ϕ_u has generated some discussion (Scarrott 2015; Hu 2013). A special case of [4] is where $\phi_u = 1 - H(u \mid \theta_b)$. This will be referred to as the "bulk model-based tail fraction model" (BTFM). A benefit of this approach is that it borrows information from the "bulk model" which usually has ample data. A majority of spliced models adopt this approach, and it is advantageous when the "bulk model" is known to be correct. However, it may be inappropriate in scenarios where the bulk model is not a good descriptor of the tail (Scarrott 2015).

The tail fraction ϕ_u can also be considered as an additional model parameter which controls the probability of coming from the tail distribution. Hu (2013) shows that this

approach provides more flexibility and is clearly better than the BTFM when the "bulk model" is mis-specified. Scarrott (2015) shows that the maximum likelihood estimator of the tail fraction is the sample proportion of excesses, i.e., $\hat{\phi}_u = \frac{n_u}{n}$, where n_u is the number of excesses above the threshold u and n is the sample size. Fixing $\hat{\phi}_u = \frac{n_u}{n}$ in (4) will be referred to as the "Parameterized Tail Fraction Model" (PTFM).

Although the above model specifications guarantee a continuous CDF, the PDF is not necessarily continuous. Scarrott (2015) gives a simple approach to constrain the pdf to be continuous at the threshold u. The right limit of the GPD pdf evaluated at the threshold u is equated to the bulk model pdf evaluated at the threshold giving the following restriction on the GPD scale parameter σ_u . For the BTFM,

$$\sigma_u = \frac{1 - H(u \mid k, \theta)}{h(u \mid k, \theta)}$$

and for the PTFM,

$$\sigma_u = \frac{H(u \mid k, \theta)}{1 - \phi_u} \frac{\phi_u}{h(u \mid k, \theta)}$$

Under this constraint, σ_u does not have to be estimated in either the BTFM or the PTFM. The R package evmix was used to specify the spliced kernels (Scarrott and Hu 2017).

3. PARAMETER ESTIMATION

3.1. APPROXIMATION OF THE LIKELIHOOD IN THE RESOURCE SELECTION MODEL (RSM)

A major hurdle in fitting the RSM (1) is the evaluation of the intractable normalizing constant $C(\mathbf{s}_i, \boldsymbol{\beta}, \boldsymbol{\theta}) = \int_{S} e^{\mathbf{x}'(\mathbf{z})\boldsymbol{\beta}} q(\mathbf{z}; \mathbf{s}_i, \boldsymbol{\theta}) d\mathbf{z}$.

It is clear that $C(\mathbf{s}_i, \boldsymbol{\beta}, \boldsymbol{\theta})$ can be expressed as the expectation $E_q(\mathbf{e}^{\mathbf{x}'(\mathbf{z})\boldsymbol{\beta}})$, where $q(\mathbf{z}; \mathbf{s}_i, \boldsymbol{\theta})$ is the PDF of the end location \mathbf{z} , ignoring any resource selection. We thus consider a Monte Carlo approximation to C, with

$$C(\mathbf{s}_i, \boldsymbol{\beta}, \boldsymbol{\theta}) \approx \frac{\sum_{j=1}^N e^{\mathbf{x}'(\mathbf{z}_j)\boldsymbol{\beta}}}{N}, \quad \mathbf{z}_j \stackrel{\text{iid}}{\sim} q(\mathbf{z}; \mathbf{s}_i, \boldsymbol{\theta}).$$

Each end location \mathbf{z}_j is obtained by simulating a distance d_j from the distance kernel q (this is done by the inverse CDF method), simulating a bearing φ_j from a uniform circular distribution and then using the transformation $\mathbf{z}_j = (s_{i,1} + d_j \cos(\varphi_j), s_{i,2} + d_j \sin(\varphi_j))$ to obtain the resulting end location. N is the Monte Carlo sample size.

When covariates are not considered, the normalizing constant reduces to $C(\mathbf{s}_i, \boldsymbol{\theta}) = \int_{S} q(\mathbf{z}; \mathbf{s}_i, \boldsymbol{\theta}) d\mathbf{z}$. The Monte Carlo approximation in this case is

$$C(\mathbf{s}_i, \boldsymbol{\theta}) \approx \frac{\sum_{j=1}^{N} I(\mathbf{z}_j \in S)}{N}, \quad \mathbf{z}_j \stackrel{\text{iid}}{\sim} q(\mathbf{z}; \mathbf{s}_i, \boldsymbol{\theta}).$$

where $I(\mathbf{z}_j \in S)$ is an indicator function with value 1 if the simulated end location \mathbf{z}_j falls in the region of interest S and 0 otherwise.

Note that $C(\mathbf{s}_i, \boldsymbol{\beta}, \boldsymbol{\theta})$ is different for each start location i, so we must approximate $C(\mathbf{s}_i, \boldsymbol{\beta}, \boldsymbol{\theta})$ for each of the 704 start locations in the yearly movement data. We parallelized this operation using the parallel package in R (R Core Team 2016).

3.2. BAYESIAN FRAMEWORK AND MCMC

We adopt a Bayesian approach for model estimation similar to Behrens et al. (2004). We specify diffuse prior distributions for all parameters. The Gamma distribution shape and scale parameters k and θ are estimated on the log scale. We use N(0, 100) priors for the feature covariates $\beta_0, \beta_1, \ldots, \beta_p$, $\log(k)$, $\log(\theta)$ and the shape parameter ξ of the GPD. Samples from the posterior distribution are drawn using a Markov Chain Monte Carlo (MCMC) algorithm. All parameters are updated jointly using Metropolis–Hastings steps, and we use adaptive tuning (Roberts and Rosenthal 2009) to tune the random walk proposal variance. A critical step in using the spliced model is specifying the threshold u. It is often problematic to estimate this parameter jointly with other model parameters (Scarrott and MacDonald 2012). We tried estimating this jointly with other model parameters with little success (results not shown). Behrens et al. (2004) do this and warn that the threshold is difficult to estimate in this manner. In this study, we used a mean excess plot (Davison and Smith 1990) to guide our choice in picking several candidate thresholds and then used goodness-of-fit techniques to select the best u. Candidate thresholds were picked by looking for linearity above the threshold and by considering a range of reasonable quantiles.

The method we used approximates the likelihood using a Monte Carlo estimate within a MCMC sampler; it stores the current value of the likelihood without re-sampling or approximating it afresh at each iteration. This method falls into the framework of a grouped independence metropolis—hastings (GIMH) sampler introduced by Beaumont (2003). A generalization of this sampler together with theoretical results that discuss the convergence properties of it is given in Andrieu and Roberts (2009).

We note that the denominator of the approximation of the likelihood is unbiased for the denominator of the actual likelihood, but this does not guarantee the approximation is unbiased for the entire likelihood. In order to assess if this in fact induces a systematic bias in our parameter estimation, we conducted a simulation study in which we considered an RSM with a Gamma distance kernel and one covariate, elevation, and simulated 1000 data sets with fixed true parameters. The details can be found in Appendix B. The distributions of the MAP estimates are given in Fig. 6, which demonstrates that there is no trace of systematic bias in the estimation, although the likelihood itself is biased. We did a second simulation in which we simulated movement data based on Gamma, PTFM and BTFM distance kernels, and attempted to recover the true parameter values. We used a single covariate (elevation) in this study. The posterior distributions for the parameters captured the true parameters very well for all three types of kernels. See Fig. 7.

Beaumont (2003) notes that taking larger Monte Carlo sample sizes leads to better MCMC convergence. We found that the number of Monte Carlo samples used had a large impact on how well the chains mixed. Larger Monte Carlo sample sizes lead to lower variance of

the likelihood estimation and better mixing of the MCMC sampler. More complex models such as the models that included covariates and a spliced distance kernel needed a higher number of samples to achieve a similar variance than simpler models which did not include covariates. We decided on having the same number of samples across all the models to facilitate comparison and chose a Monte Carlo sample size of N=30,000, which gave a standard deviation of approximately 0.1 using 10 replicates for the likelihood of the most complex models. We ran the MCMC sampler for 50,000 iterations for each model and checked convergence visually using trace plots. The computing times in minutes for running the chains are given in Table 1. The cluster used 3 dual 10-core Xeon E5-2680 processors run in a Red Hat Enterprise Linux 6 computing environment. The computer code can be found in the supplementary materials.

3.3. APPLICATION TO ELK YEARLY MOVEMENTS

We used the deviance information criterion (DIC) (Spiegelhalter et al. 2002) and cross-validated log scores (Gneiting and Raftery 2007) for model comparison. For cross-validation, we divided the data set into training (80%) and testing (20%) sets, obtained posterior distributions using the training set and calculated the cross-validation score based on the posterior samples and the log-likelihood of the testing set as

CV Score =
$$\sum_{k=1}^{K} E(\log[\mathbf{e}_k \mid \mathbf{s}_k, \boldsymbol{\theta}]) \approx \sum_{k=1}^{K} \frac{1}{M} \sum_{j=1}^{M} \log[\mathbf{e}_k \mid \mathbf{s}_k, \boldsymbol{\theta}_j]$$

K is the number of data points in the testing set, M the number of posterior samples, and θ_i the posterior samples of the parameters from the jth iteration of the chain.

4. RESULTS

4.1. MODEL COMPARISON

We considered fourteen different models based on the form of the distance kernel, the threshold used, and whether the feature covariates were included or not. The thresholds we picked were u=10,13 and 27 corresponding to the 66th, 75th and 90th empirical percentiles of the yearly movements distribution. The mean excess plot given in Fig. 3 guided our choice of thresholds. Our goal was not to pick the optimal threshold, as this is very difficult to do, but to pick several thresholds and use model comparison methods to pick the best model.

We present the DIC and cross-validation scores for each model together with the computing time (in minutes) in Table 1. Models with Gamma distance kernels had much lower computing times compared to the models with spliced distance kernels. Cross-validation scores of -Inf denote models where the posterior distributions of the parameters lead to zero likelihood of some of the data points in the test set. This occurs when the parameter estimates specify a finite tail for the movements, and there are test points that exceed the estimated maximum distance. Based on DIC and the cross-validation score, we found that

Model no.	Covariates	Distance kernel	и	DIC	C.V. score	Comp. time (min)
1	No	Gamma	NA	15414.6	- 1503.2	565
2	No	BTFM	10	15396.0	- 1499.7	4858
3	No	BTFM	13	15400.4	-1500.2	4782
4	No	BTFM	27	15413.2	-1503.0	4924
5	No	PTFM	10	15378.7	-Inf	4928
6	No	PTFM	13	15377.8	-Inf	4969
7	No	PTFM	27	15386.3	-Inf	5034
8	Yes	Gamma	NA	15308.2	-1495.0	700
9	Yes	BTFM	10	15299.1	-1493.0	4462
10	Yes	BTFM	13	15300.8	-1493.4	5406
11	Yes	BTFM	27	15308.7	-1495.1	5079
12	Yes	PTFM	10	15290.5	- 1491.1	4720
13	Yes	PTFM	13	15290.8	-1491.6	4632
14	Yes	PTFM	27	15290.9	-1491.8	5404

Table 1. Model comparison.

The best model with covariates and without covariates are given in bold

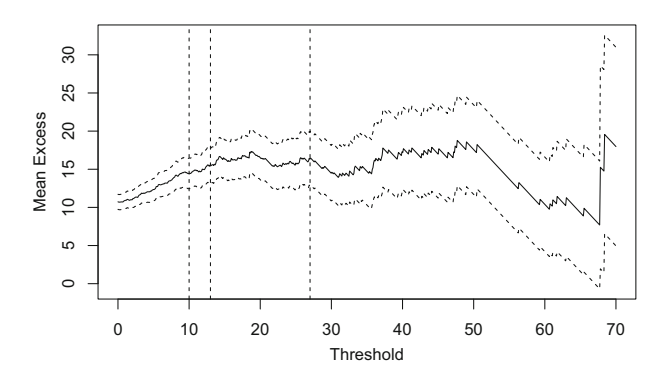


Figure 3. Mean excess plot for yearly movements. We considered thresholds of u=10, 13 and 27, shown as vertical dashed lines.

Model 12 was the best model overall. We also found that Model 2 was the best model when resource selection is not considered.

4.2. PARAMETER ESTIMATES

We give the parameter estimates for Models 12, 2 and 5 in Table 2. Model 12 is the best model overall, and Model 2 is the best model when no covariates are considered. We also give the parameter estimates for Model 5, which has the same distance kernel as Model 12 but does not account for resource selection. We present the parameter estimates for Model 5 to see the effect of including the resource selection component. We obtain Monte Carlo standard error using the batchmeans package in R (Haran and Hughes 2016). For all three models, we obtained positive point estimates for the shape parameter ξ of the GPD with the 95% equal tailed credible intervals for ξ not overlapping zero in both models. A positive ξ denotes a heavy tail. However, we see that including the covariates accounts for some of the

Model	Parameter	Mode	Mean	LL	UL	MCMC S.E.
12	Agricultural land Elevation	- 0.44 0.18	- 0.45 0.21	- 0.75 - 0.27	-0.18 0.65	0.0075 0.0150
	Elevation ²	-0.83	-0.85	-1.13	-0.53	0.0090
	Forest cover	-0.19	-0.19	-0.35	-0.04	0.0033
	Major roads	0.01	0.02	-0.08	0.12	0.0015
	Private/public land	0.02	0.03	-0.12	0.19	0.0032
	Road density	-0.04	-0.04	-0.18	0.10	0.0026
	Terrain roughness	0.13	0.13	-0.05	0.30	0.0036
	Water	-0.01	-0.05	-0.26	0.13	0.0040
	$\log(k)$	0.19	0.21	0.08	0.35	0.0034
	$\log(\theta)$	1.58	1.60	1.35	1.88	0.0072
	ξ	0.13	0.14	0.01	0.30	0.0031
2	$\log(k)$	-0.01	0.00	-0.11	0.10	0.0013
	$\log(\theta)$	2.23	2.24	2.08	2.41	0.0022
	ξ	0.30	0.35	0.19	0.55	0.0025
5	log(k)	0.19	0.20	0.06	0.34	0.0022
	$\log(\theta)$	1.54	1.56	1.33	1.85	0.0043
	٤	0.15	0.15	0.00	0.33	0.0021

Table 2. Parameter Estimates for Models 12, 2 and 5. Point and interval estimates are rounded to the nearest second decimal.

Significant covariates are given in bold

heavy-tailed behavior of the movements, as the point estimates for ξ are slightly lower in Model 12 compared to Model 5. Considering Model 12, we found that the 95% equal tailed credible intervals for resource selection function parameters corresponding to agricultural land, elevation and percent forest cover do not overlap zero, indicating that elk prefer lesser values for agricultural land and forest cover. Interpretation of the coefficients for elevation has to be done with more caution due to the inclusion of the quadratic term. We found that elk prefer mid-level elevation by plotting the function $\exp(\beta_{elev}x + \beta_{elev}^2x^2)$ with x taking values from the range of elevation seed in the GYE.

4.3. SIMULATION OF SPREAD

To illustrate the differences between our fitted models, and the importance of modeling both resource selection and heavy-tailed movements, we conducted a simulation of the spread of an infectious disease across our study system using the best model with and without covariates, Models 12 and 2 respectively. We assume that the elk within a grid cell are well mixed (all can contact all others with equal probability) and that elk do not recover and are always infectious after contracting the disease. These assumptions are not meant to exactly replicate the spread of Brucella in GYE elk, but instead are meant to clearly illustrate how movement behavior can affect the spread of the disease.

At each time point in our simulation, we allow the infected elk population to first grow and then spread spatially across the GYE. For the growth step, we use a logistic growth model (Bacaër 2011). The differential equation for the infected population P(t) at time t is

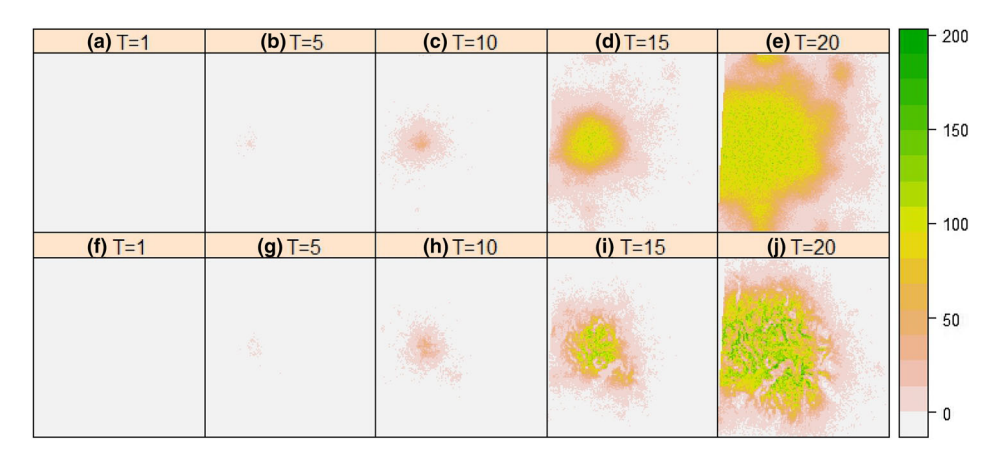


Figure 4. \mathbf{a} — \mathbf{e} gives the simulation of disease spread using a logistic growth model for time points T = 1, 5, 10, 15 and 20 using parameter estimates of Model 2. \mathbf{f} — \mathbf{j} gives the simulation of the spread for the same times using parameter estimates of Model 12. Model 12 accounts for resource selection, but Model 2 does not.

$$\frac{\mathrm{d}\mathbf{P}(t)}{\mathrm{d}t} = r\mathbf{P}(t)\left(1 - \frac{\mathbf{P}(t)}{K}\right)$$

where r is the growth rate and K the carrying capacity. The solution for this differential equation is

$$\mathbf{P}(t) = \frac{K\mathbf{P}(t-1)\exp^{r\Delta t}}{K + \mathbf{P}(t-1)(\exp^{r\Delta t} - 1)}$$

where Δt is a time interval (Bacaër 2011). We used K = 100 as the carrying capacity and r = 1.05 as the growth rate.

From the growth step, we obtained the number of infected elk in each grid cell at time t. In the propagate step, we then simulated an end cell for each infected elk. The elk are allowed to move freely without a restriction on the number of elk within a landscape cell. For the model without covariates (Model 2), this was simply done by simulating a bearing and a distance for each elk individual using the parameter estimates and obtaining its end location. For the model with covariates (Model 12), we did this by first simulating 1000 bearings and distances from the current location of each elk using our parameter estimates, weighting each movement by $w_j = \exp(\mathbf{X}(j)\boldsymbol{\beta})$, and sampling an end location based on these weights. The simulation was carried out for 20 time steps. We present the spread at time points 1, 5, 10, 15 and 20 in Fig. 4.

4.4. DISCUSSION OF SIMULATION STUDY RESULTS

For both simulations in Fig. 4, we can see long-range movements in the spread of the disease. When comparing the spread in Fig. 4, we can see that the disease seems to spread faster when resource selection is not considered. This is further illustrated in Fig. 5, where the number of landscape cells infected through time is greater when Model 2 is used. However, looking at the lower panel in Fig. 4, we can see that the density of infected elk is patchy.

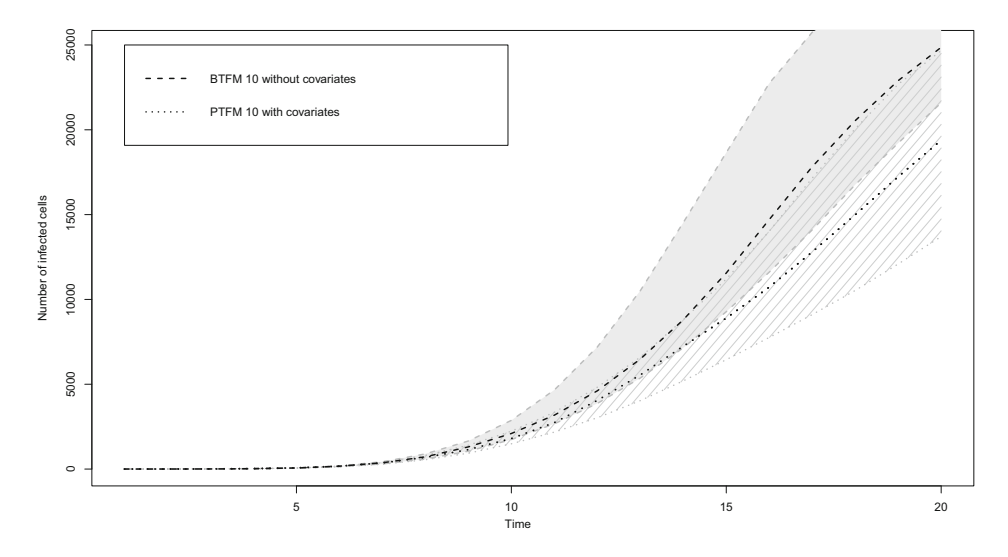


Figure 5. The dotted and dashed lines give the number of landscape cells infected through time for simulations based on Model 12 and Model 2, respectively. We sampled 1000 parameter values post-burn-in and ran the simulation of spread for each. 90% credible regions are given with dashed gray lines and solid gray color for Models 12 and 2, respectively. Spread using Model 2 is faster.

There are pockets of high infection, corresponding to patches of habitat that are highly preferred by GYE elk in the winter months.

5. DISCUSSION

5.1. MAJOR FINDINGS

Unlike previous studies, we have simultaneously allowed for movement kernels to be both heavy-tailed and a function of landscape covariates. We found that the movement kernel is not solely a function of the animal species, but is an interaction between the animal and its environment, whereby increased habitat patchiness is likely to result in slower invasion speeds. This result is contrary to early studies, which suggest that heavier-tailed distributions will result in faster wave speeds (Clark 1998; Kot et al. 1996) and similar to the findings of Urban et al. (2008) and Lindström et al. (2011). We found that in the presence of habitat selection, the distance kernel of elk became less heavy-tailed as movements were biased toward closer preferred habitats.

In this study, we modeled the yearly movement of elk by simultaneously considering resource selection and extreme movements by using a resource selection function and a spliced dispersal kernel. We found that some of the heavy tail behavior seen when resource selection is not considered is accounted for when it is included. We found that the PTFM model with a threshold of u=10 was the best fitting model and that elk prefer less agricultural lands and forest cover and medium elevation in winter months.

Resource selection has two important effects. Firstly, it clusters animals in good terrain, and this will make density-dependent diseases spread faster locally. Secondly, resource

selection can make spatial transmission slower; as in some habitat scenarios, including the landscape of the GYE, movements between patches of good terrain are separated by large enough distances that only very rarely will individuals move to a new patch of good terrain. The simulation study was meant to explore the second aspect in particular and illustrates that spatial spread of disease may be slowed by resource selection. In order to investigate the effect of including a resource selection function in a movement model, we compared the simulation of disease spread using two models: one that included resource selection (Model 12) and one that did not (Model 2). We found that including resource selection affected the nature of spread of the disease with more patchy spread than a more uniform spread when resource selection is not considered. Also we found that there was a difference in the speed of disease spread with the model that did not include resource selection, showing higher speeds of spread. We believe this provides motivation to include a resource selection component when modeling the spread of infectious diseases through patchy habitat.

5.2. FUTURE WORK

The intractable normalizing constant in our weighted distribution model makes inference computationally expensive. This impedes the use of this model for very large datasets. Future work will consider ways to lower the computing costs, including using graphics processing units (GPUs) to compute the Monte Carlo estimate of the normalizing constant.

When fitting the spliced distributions, we did not attempt to find an optimal threshold u. Instead, we chose two thresholds and then used model selection techniques to choose between them. Obtaining an optimal threshold was not computationally feasible. A possibility to circumvent this issue could be to specify a distance kernel that has flexibility in its tails but does not need the specification of a threshold, similar to that given in Naveau et al. (2016).

We considered only a fixed resource selection model. Different functional forms of the covariates can be easily included within this framework; however, the primary objective of this paper was not to find the "best" possible model to explain elk movement. In the future, we will explore ways to do variable selection for the covariates in a computationally efficient manner, through Bayesian regularization priors, such as the Bayesian LASSO (Park and Casella 2008). In addition, a full analysis of the effects of resource selection, heavy-tailed movement, and disease dynamics is the subject of the ongoing research.

Our approach successfully models both resource selection and heavy-tailed movements, allowing for a more complete understanding of how disease might spread through a population of animals when preferred resources are scarce. Capturing the interplay of these two processes will allow for more accurate prediction of future spread of brucellosis in the GYE, and the future progression of invasions in a wide range of wildlife systems.

ACKNOWLEDGEMENTS

We gratefully acknowledge financial support from DOE DE-AC02-05CH11231, USGS G16AC00055, NSF EEID 1414296, NIH GM116927-01, NSF MRI-1626251, NSF DMS-1752280 and NSF DEB-1245373. Computations for this research were performed on the Pennsylvania State University's Institute for CyberScience Advanced

CyberInfrastructure (ICS-ACI). This content is solely the responsibility of the authors and does not necessarily represent the views of the Institute for CyberScience. We thank Montana, Fish, Wildlife and Parks, Idaho Department of Fish and Game, Wyoming Game and Fish Department, Yellowstone and Grand Teton National Parks, US Fish and Wildlife Service, and Wildlife Conservation Society for providing elk location data. Any mention of trade, product or firm names is for descriptive purposes only and does not imply endorsement by the US Government.

[Received January 2018. Accepted October 2018. Published Online November 2018.]

APPENDIX A: TREATMENT OF MISSING VALUES

We encountered missing values in certain landcover rasters. Aggregating the raster reduced the number of missing values significantly. We observed that missing values were in landscape cells that fell on the boundaries of certain rasters (this is clearly seen in Fig. 2). We also noted that landscape cells with missing values were far away from the region where we observed elk movements. We used a 27×27 grid to interpolate the value of a missing landscape cell. We weighted the grid giving landscape cells closer to the missing landscape cell higher weights than those further away.

APPENDIX B: SIMULATION STUDY TO TEST BIAS IN ESTIMATION

In order to check if there is a systematic bias induced by approximating the normalizing constant using a Monte Carlo approximation, we conducted a simulation study with a single covariate (Elevation) and a gamma distance kernel. We set the true parameter values to $(\beta, k, \theta) = (-1, 0.8615017, 12.63035)$. We simulated 1000 datasets each with 200 yearly movements where the start locations for the 200 movements were chosen randomly from the 704 movements in the dataset. We simulated from our model using importance sampling. We first simulated many end locations \mathbf{e}_i for each start location by simulating bearings and distances from the distance kernel. We then sampled a single end location drawn randomly from the simulated end locations, with probabilities proportional to $e^{x(e_i)\beta}$. After simulating 200 yearly movements in this way, we estimated model parameters using the Bayesian method given in Sect. 3. We used 2500 Monte Carlo samples to approximate the normalizing constant. We fit the model to the simulated data running the MCMC sampler for 30,000 iterations and removed the first 5000 runs as burn in. We obtained the posterior mode for each parameter from each dataset and plotted their densities in Fig. 6. The true values are given using a solid vertical line. It is clearly evident from Fig. 6 that there is very little systematic bias induced when using the proposed estimation procedure.

We also simulated 3 datasets using gamma and spliced distance kernels. The true parameters used were $(\beta, k, \theta) = (-1, 0.8615017, 12.63035)$ and $\xi = 0.2$ with u = 10 and $\phi_u = 0.3$. The start locations were taken to be those of the actual data. We simulated the end locations similarly to that given above using the relevant distance kernel. We used 5000 Monte Carlo samples in the likelihood estimation. The results are given in Fig. 7. We found that all the true parameters were captured well giving us the assurance that the estimation procedure does well for models with spliced kernels too.

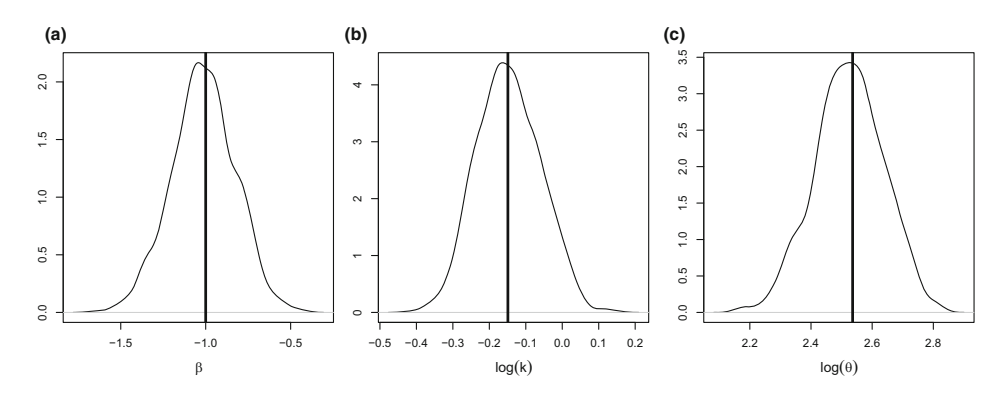


Figure 6. The distributions of posterior modes for the parameters \mathbf{a} β , \mathbf{b} $\log(k)$ and \mathbf{c} $\log(\theta)$ for models with a fixed covariate elevation and a gamma distance kernel. The true values of the parameters are $\beta = -1$, $\log(k) = -0.1490782$ and $\log(\theta) = 2.536103$. There is no evidence of an estimation bias.

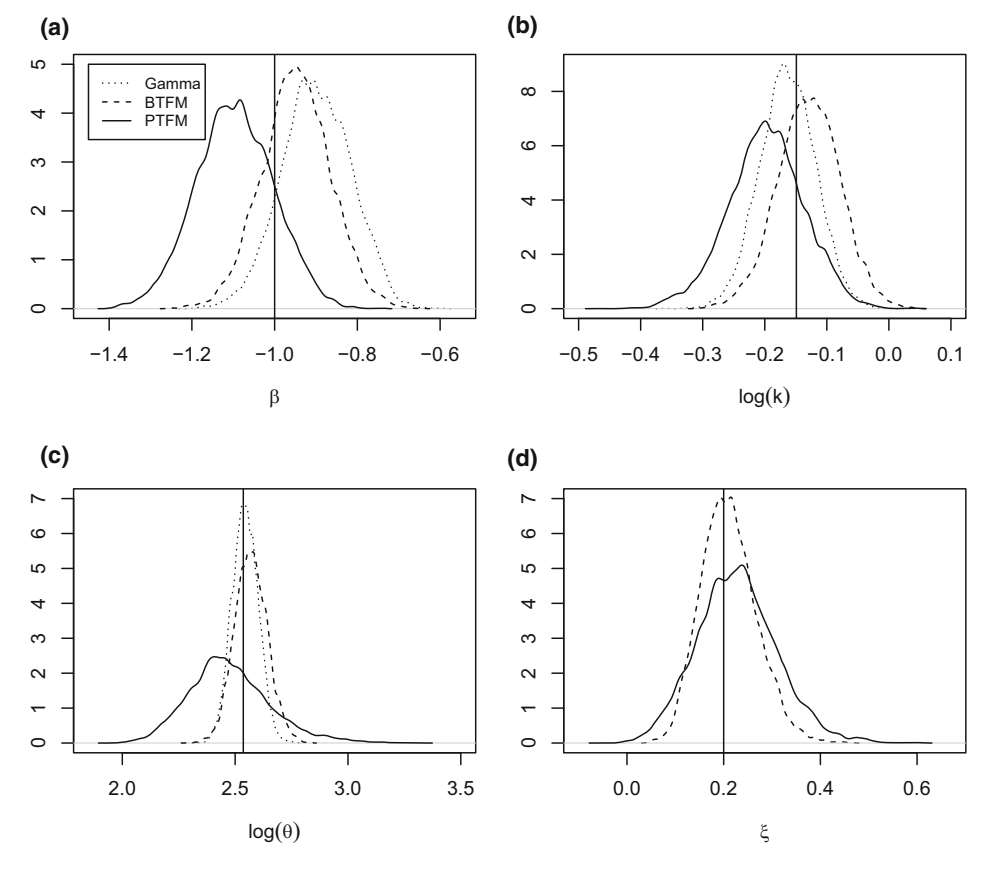


Figure 7. The posterior distributions of the parameters \mathbf{a} β , \mathbf{b} $\log(k)$, \mathbf{c} $\log(\theta)$ and \mathbf{d} ξ for models with a fixed covariate elevation and a Gamma distance kernel (dotted line), a BTFM distance kernel (dashed line) and a PTFM distance kernel (solid line). The true values of the parameters are $\beta = -1$, $\log(k) = -0.1490782$, $\log(\theta) = 2.536103$ and $\xi = 0.2$.

REFERENCES

- Andrieu, C., and Roberts, G. O. (2009), "The pseudo-marginal approach for efficient Monte Carlo computations," Ann. Statist., 37(2), 697–725. https://doi.org/10.1214/07-AOS574
- Avgar, T., Potts, J. R., Lewis, M. A., and Boyce, M. S. (2016), "Integrated step selection analysis: bridging the gap between resource selection and animal movement," *Methods in Ecology and Evolution*, 7(5), 619–630. http://onlinelibrary.wiley.com/doi/10.1111/2041-210X.12528/abstract
- Bacaër, N, N. (1838), "Verhulst and the logistic equation (1838)," in *A Short History of Mathematical Population Dynamics*, London: Springer London, pp. 35–39. http://webpages.fc.ul.pt/~mcgomes/aulas/dinpop/Mod13/Verhulst.pdf
- Beaumont, M. A. (2003), "Estimation of Population Growth or Decline in Genetically Monitored Populations," *Genetics*, 164(3), 1139–1160. http://www.genetics.org/content/164/3/1139
- Behrens, C. N., Lopes, H. F., and Gamerman, D. (2004), "Bayesian analysis of extreme events with threshold estimation," *Statistical Modelling*, 4(3), 227–244. https://doi.org/10.1191/1471082X04st075oa
- Clark, J. S. (1998), "Why Trees Migrate So Fast: Confronting Theory with Dispersal Biology and the Paleorecord," The American Naturalist, 152(2), 204–224 http://www.jstor.org/stable/10.1086/286162
- Clark, J. S., Lewis, M., McLachlan, J. S., and HilleRisLambers, J. (2003), "Estimating Population Spread: What Can We Forecast and How Well?," *Ecology*, 84(8), 1979–1988. http://onlinelibrary.wiley.com/doi/10.1890/ 01-0618/abstract
- Clark, J. S., Silman, M., Kern, R., Macklin, E., and HilleRisLambers, J. (1999), "Seed Dispersal Near and Far: Patterns Across Temperate and Tropical Forests," *Ecology*, 80(5), 1475–1494. http://onlinelibrary.wiley.com/doi/10.1890/0012-9658(1999)080[1475:SDNAFP]2.0.CO;2/abstract
- Coulon, A., Morellet, N., Goulard, M., Cargnelutti, B., Angibault, J.-M., and Hewison, A. (2008), "Inferring the effects of landscape structure on roe deer (Capreolus capreolus) movements using a step selection function," *Landscape Ecology*, 23(5), 603–614. https://link.springer.com/article/10.1007/s10980-008-9220-0
- Cross, P. C., Maichak, E. J., Rogerson, J. D., Irvine, K. M., Jones, J. D., Heisey, D. M., Edwards, W. H., and Scurlock, B. M. (2015), "Estimating the phenology of elk brucellosis transmission with hierarchical models of cause-specific and baseline hazards," *Journal of Wildlife Management*, 79(5), 739–748. https://wildlife. onlinelibrary.wiley.com/doi/abs/10.1002/jwmg.883
- Davison, A. C., and Smith, R. L. (1990), "Models for Exceedances over High Thresholds," *Journal of the Royal Statistical Society. Series B (Methodological)*, 52(3), 393–442. http://www.jstor.org/stable/2345667
- Forester, J. D., Im, H. K., and Rathouz, P. J. (2009), "Accounting for animal movement in estimation of resource selection functions: sampling and data analysis," *Ecology*, 90(12), 3554–3565. http://onlinelibrary.wiley.com/ doi/10.1890/08-0874.1/abstract
- Garcí-a, C., and Borda-de Água, L. (2017), "Extended dispersal kernels in a changing world: insights from statistics of extremes," *Journal of Ecology*, 105(1), 63–74. https://doi.org/10.1111/1365-2745.12685
- Gneiting, T., and Raftery, A. E. (2007), "Strictly proper scoring rules, prediction, and estimation," *J. Amer. Statist. Assoc.*, 102(477), 359–378. https://doi.org/10.1198/016214506000001437
- Hanks, E. M., Hooten, M. B., and Alldredge, M. W. (2015), "Continuous-time discrete-space models for animal movement," *Ann. Appl. Stat.*, 9(1), 145–165. https://doi.org/10.1214/14-AOAS803
- Haran, M., and Hughes, J. (2016), batchmeans: Consistent Batch Means Estimation of Monte Carlo Standard Errors, Denver, CO. R package version 1.0-3.
- Hijmans, R. J. (2016), raster: Geographic Data Analysis and Modeling. R package version 2.5-8. https://CRAN. R-project.org/package=raster
- Hooten, M. B., Hanks, E. M., Johnson, D. S., and Alldredge, M. W. (2013), "Reconciling resource utilization and resource selection functions," *Journal of Animal Ecology*, 82(6), 1146–1154. http://pubs.er.usgs.gov/ publication/70192618
- Hooten, M. B., Johnson, D. S., Hanks, E. M., and Lowry, J. H. (2010), "Agent-Based Inference for Animal Movement and Selection," *Journal of Agricultural, Biological and Environmental Statistics*, 15(4), 523–538. https://doi.org/10.1007/s13253-010-0038-2

- Hooten, M. B., Johnson, D. S., McClintock, B. T., and Morales, J. M. (2017), Animal movement: Statistical models for telemetry data CRC Press. http://pubs.er.usgs.gov/publication/70192618
- Hu, Y. (2013), Extreme Value Mixture Modelling with Simulation Study and Applications in Finance and Insurance, Master's thesis, University of Canterbury, New Zealand. http://www.math.canterbury.ac.nz/~c.scarrott/evmix/ thesis.pdf
- Johnson, D. S., Thomas, D. L., Ver Hoef, J. M., and Christ, A. (2008), "A General Framework for the Analysis of Animal Resource Selection from Telemetry Data," *Biometrics*, 64(3), 968–976. http://onlinelibrary.wiley.com/doi/10.1111/j.1541-0420.2007.00943.x/abstract
- Kamath, P. L., Foster, J. T., Drees, K. P., Luikart, G., Quance, C., Anderson, N. J., Clarke, P. R., Cole, E. K., Drew, M. L., Edwards, W. H., Rhyan, J. C., Treanor, J. J., Wallen, R. L., White, P. J., Robbe-Austerman, S., and Cross, P. C. (2016), "Genomics reveals historic and contemporary transmission dynamics of a bacterial disease among wildlife and livestock," *Nature Communications*, 7, 11448. https://doi.org/10.1038/ncomms11448
- Kot, M., Lewis, M. A., and van den Driessche, P. (1996), "Dispersal Data and the Spread of Invading Organisms," Ecology, 77(7), 2027–2042. https://www.jstor.org/stable/2265698
- Lindström, T., Håkansson, N., and Wennergren, U. (2011), The shape of the spatial kernel and its implications for biological invasions in patchy environments,, in *Proceedings of the Royal Society B: Biological Sciences*, Vol. 278, pp. 1564–1571. http://rspb.royalsocietypublishing.org/content/early/2010/11/01/rspb.2010.1902
- MacDonald, A., Scarrott, C., Lee, D., Darlow, B., Reale, M., and Russell, G. (2011), "A flexible extreme value mixture model," *Computational Statistics & Data Analysis*, 55(6), 2137–2157. http://www.sciencedirect.com/science/article/pii/S0167947311000077
- Marzluff, J. M., Millspaugh, J. J., Hurvitz, P., and Handcock, M. S. (2004), "Relating Resources to a Probabilistic Measure of Space Use: Forest Fragments and Steller's Jays," *Ecology*, 85(5), 1411–1427. https://esajournals. onlinelibrary.wiley.com/doi/abs/10.1890/03-0114
- McClintock, B. T., Johnson, D. S., Hooten, M. B., Ver Hoef, J. M., and Morales, J. M. (2014), "When to be discrete: the importance of time formulation in understanding animal movement," *Movement Ecology*, 2(1), 21. https://doi.org/10.1186/s40462-014-0021-6
- McClintock, B. T., King, R., Thomas, L., Matthiopoulos, J., McConnell, B. J., and Morales, J. M. (2012), "A general discrete-time modeling framework for animal movement using multistate random walks," *Ecological Monographs*, 82(3), 335–349. https://esajournals.onlinelibrary.wiley.com/doi/abs/10.1890/11-0326.1
- Meagher, M., and Meyer, M. E. (1994), "On the Origin of Brucellosis in Bison of Yellowstone National Park: A Review," *Conservation Biology*, 8(3), 645–653. https://doi.org/10.1046/j.1523-1739.1994.08030645.x
- Morales, J. M. (2002), "Behavior at Habitat Boundaries Can Produce Leptokurtic Movement Distributions," *The American Naturalist*, 160(4), 531–538. http://www.jstor.org/stable/10.1086/342076
- Morales, J. M., Haydon, D. T., Frair, J., Holsinger, K. E., and Fryxell, J. M. (2004), "Extracting more out of relocation data: Building movement models as mixtures of random walks," *Ecology*, 85(9), 2436–2445. https://esajournals.onlinelibrary.wiley.com/doi/abs/10.1890/03-0269
- National Academies of Sciences, Engineering, and Medicine (2017), *Revisiting Brucellosis in the Greater Yellowstone Area*, Washington, DC: The National Academies Press. https://www.nap.edu/catalog/24750/revisiting-brucellosis-in-the-greater-yellowstone-area
- Naveau, P., Huser, R., Ribereau, P., and Hannart, A. (2016), "Modeling jointly low, moderate, and heavy rainfall intensities without a threshold selection," *Water Resources Research*, 52(4), 2753–2769. https://doi.org/10. 1002/2015WR018552
- Park, T., and Casella, G. (2008), "The Bayesian Lasso," Journal of the American Statistical Association, 103(482), 681–686. https://doi.org/10.1198/016214508000000337
- R Core Team (2016), R: A Language and Environment for Statistical Computing, R Foundation for Statistical Computing, Vienna, Austria. https://www.R-project.org/
- Roberts, G. O., and Rosenthal, J. S. (2009), "Examples of Adaptive MCMC," *Journal of Computational and Graphical Statistics*, 18(2), 349–367. https://doi.org/10.1198/jcgs.2009.06134

- Scarrott, C. (2015), "Univariate Extreme Value Mixture Modeling," in Extreme Value Modeling and Risk Analysis, eds. D. K. Dey, and J. Yan, Boca Raton, Florida: Chapman and Hall/CRC, pp. 41–67. https://doi.org/10.1201/b19721-4
- Scarrott, C. J., and Hu, Y. (2017), "evmix 0.2.7: Extreme Value Mixture Modelling, Threshold Estimation and Boundary Corrected Kernel Density Estimation,". Available on CRAN. http://www.math.canterbury.ac.nz/~c.scarrott/evmix
- Scarrott, C. J., and MacDonald, A. (2012), "A review of extreme value threshold estimation and uncertainty quantification," *REVSTAT Statistical Journal*, 10(1), 33–60.
- Spiegelhalter, D. J., Best, N. G., Carlin, B. P., and Van Der Linde, A. (2002), "Bayesian measures of model complexity and fit," *Journal of the Royal Statistical Society: Series B (Statistical Methodology)*, 64(4), 583–639. http://onlinelibrary.wiley.com/doi/10.1111/1467-9868.00353/abstract
- Urban, M. C., Phillips, B. L., Skelly, D. K., and Shine, R. (2008), "A Toad More Traveled: The Heterogeneous Invasion Dynamics of Cane Toads in Australia.," *The American Naturalist*, 171(3), E134–E148. PMID: 18271722. https://doi.org/10.1086/527494